Supplementary Information

Chain aggregation dictates bimolecular charge recombination and fill factor of all-polymer blend solar cells

Ren Hagio, Hiroaki Benten,* Yunju Na, Zhiyuan Liang, Naoki Oyaizu, Junya Suzuki, Shota Kubota, Min-Cherl Jung,[1] Hirotaka Kojima,[2] and Masakazu Nakamura

Division of Materials Science, Graduate School of Science and Technology, Nara Institute of Science and Technology, Takayama-cho, Ikoma, Nara 630-0192, Japan.

[1] Present address: Division of Materials Science, Faculty of Pure and Applied Sciences, University of Tsukuba, Ibaraki 305-8577, Japan.

[2] Present address: National Institute of Technology, Maizuru College, Kyoto 625-8511, Japan.

1. *J–V* Characteristics of the thin- and thick-film devices

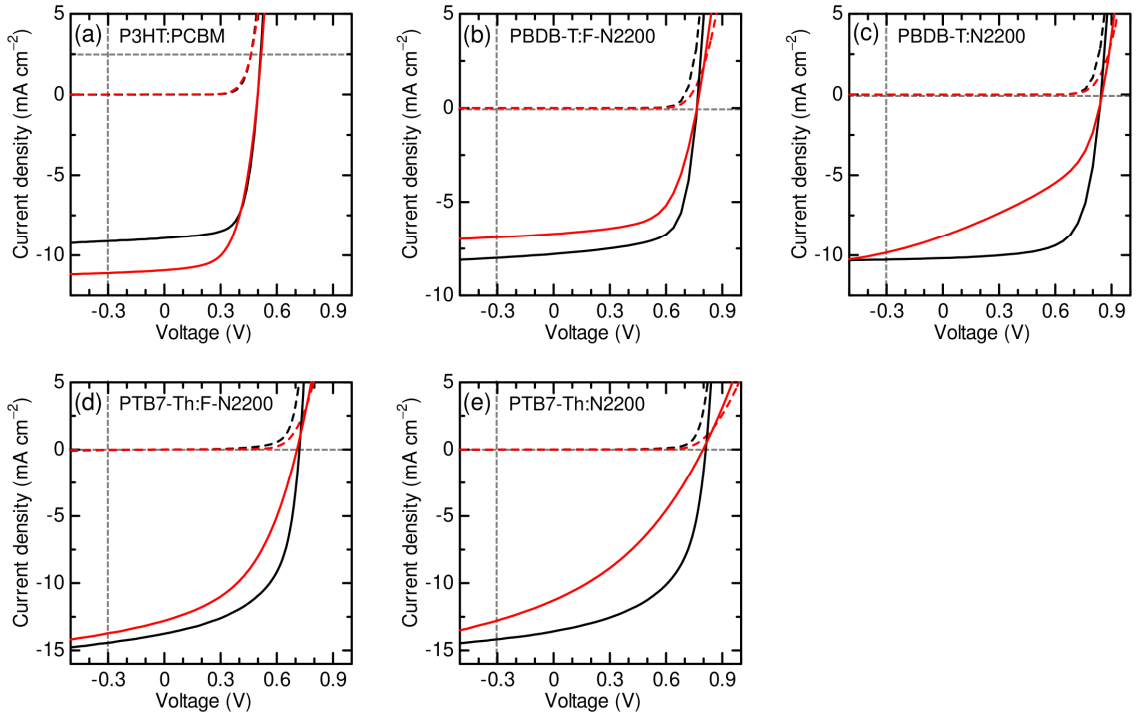

Figure S1. *J–V* characteristics of the thin-film (~100 nm, black lines) and thick-film (~300 nm, red lines) devices under AM 1.5G (100 mW cm^{-2}) illumination (solid lines) and in the dark (broken lines): (a) P3HT:PCBM (103 and 350 nm), (b) PBDB-T:F-N2200 (94 and 313 nm), (c) PBDB-T:N2200 (117 and 297 nm), (d) PTB7-Th:F-N2200 (106 and 349 nm), and (e) PTB7-Th:N2200 (86 and 301 nm).

2. Photocurrent-density (J_{ph}) characteristics of the PBDB-T:N2200 device

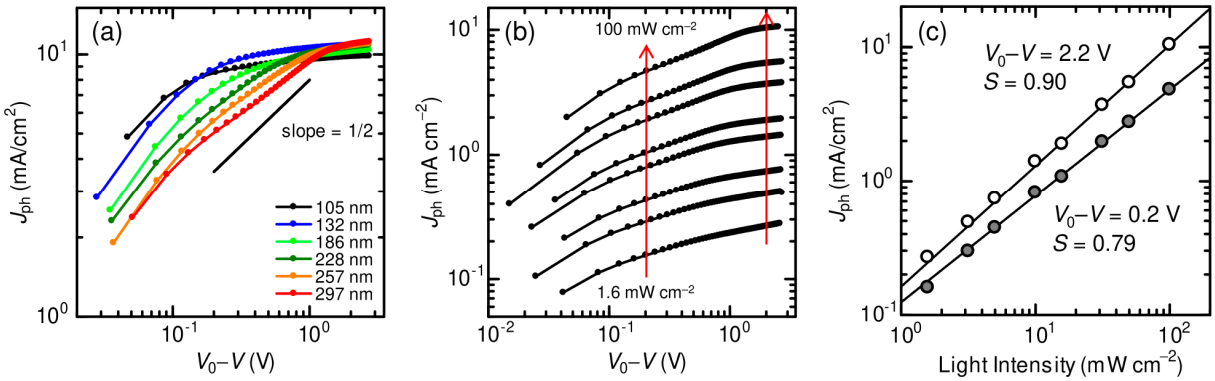

Figure S2. (a) Photocurrent density (J_{ph}) as a function of effective applied voltage (V_0–V) under a 100 mW cm^{-2} illumination for the PBDB-T:N2200 devices consisting of an active layer with a thickness of 105–297 nm. (b) Illumination light intensity dependence of J_{ph} versus V_0–V for a PBDB-T:N2200 device consisting of a 297-nm-thick active layer. (c) Illumination light intensity dependence of J_{ph} acquired from Figure S2(b) at V_0–V = 0.2 V (closed circles) and V_0–V = 2.2 V (open circles). The slope (S) determined from the linear fit (solid lines) to the experimental data is shown in the figure.

3. *J–V* characteristics of the hole- and electron-only devices

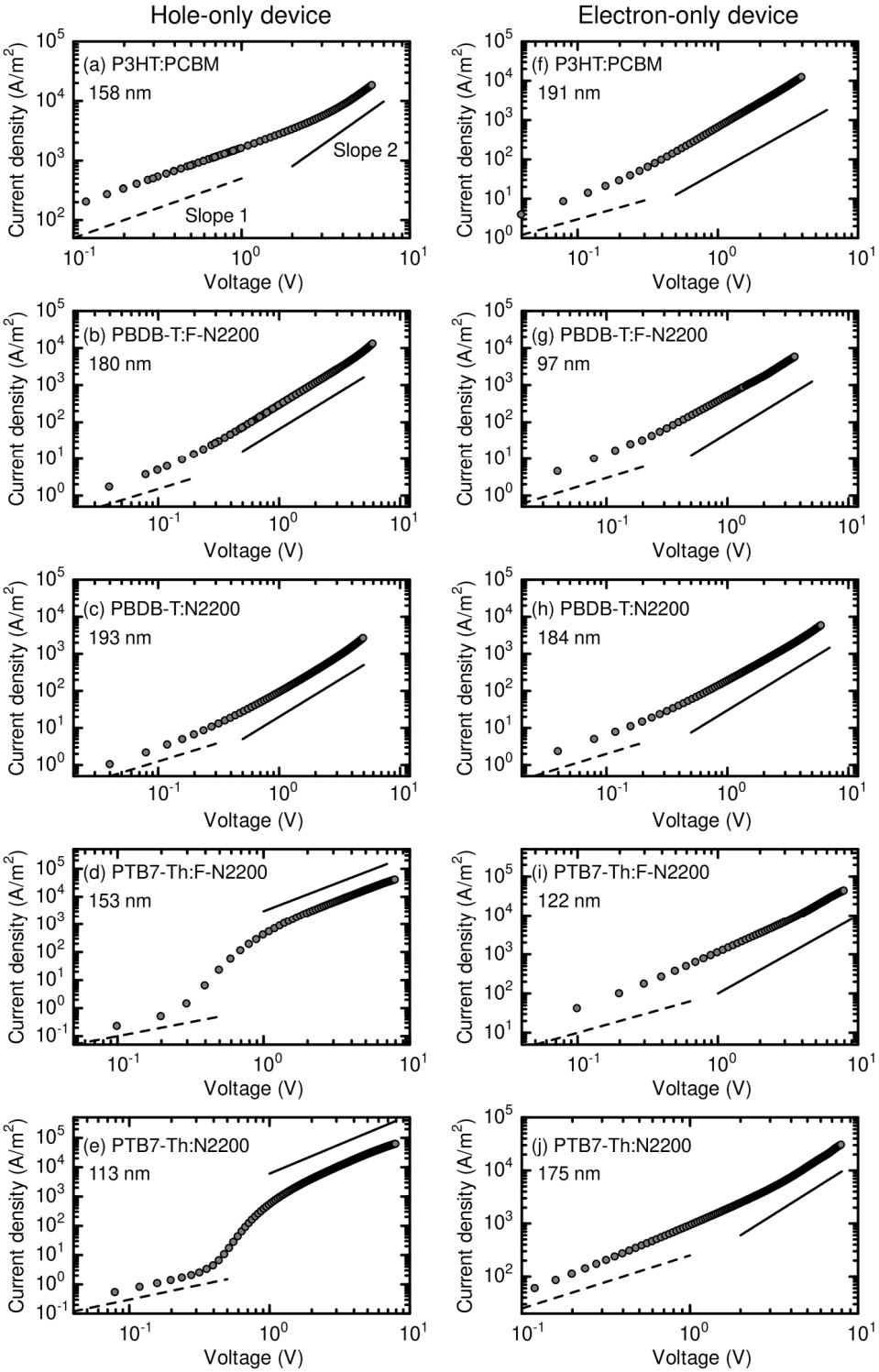

Figure S3. Dark *J–V* characteristics of the (a)–(e) hole-only and (f)–(j) electron-only devices based on (a)(f) P3HT:PCBM, (b)(g) PBDB-T:F-N2200, (c)(h) PBDB-T:N2200, (d)(i) PTB7-Th:F-N2200, and (e)(j) PTB7-Th:N2200 blend films. The solid and dashed lines represent the slopes of 2 and 1, respectively. The thickness of the blend film is indicated in each graph.

4. Electrical impedance spectroscopy results

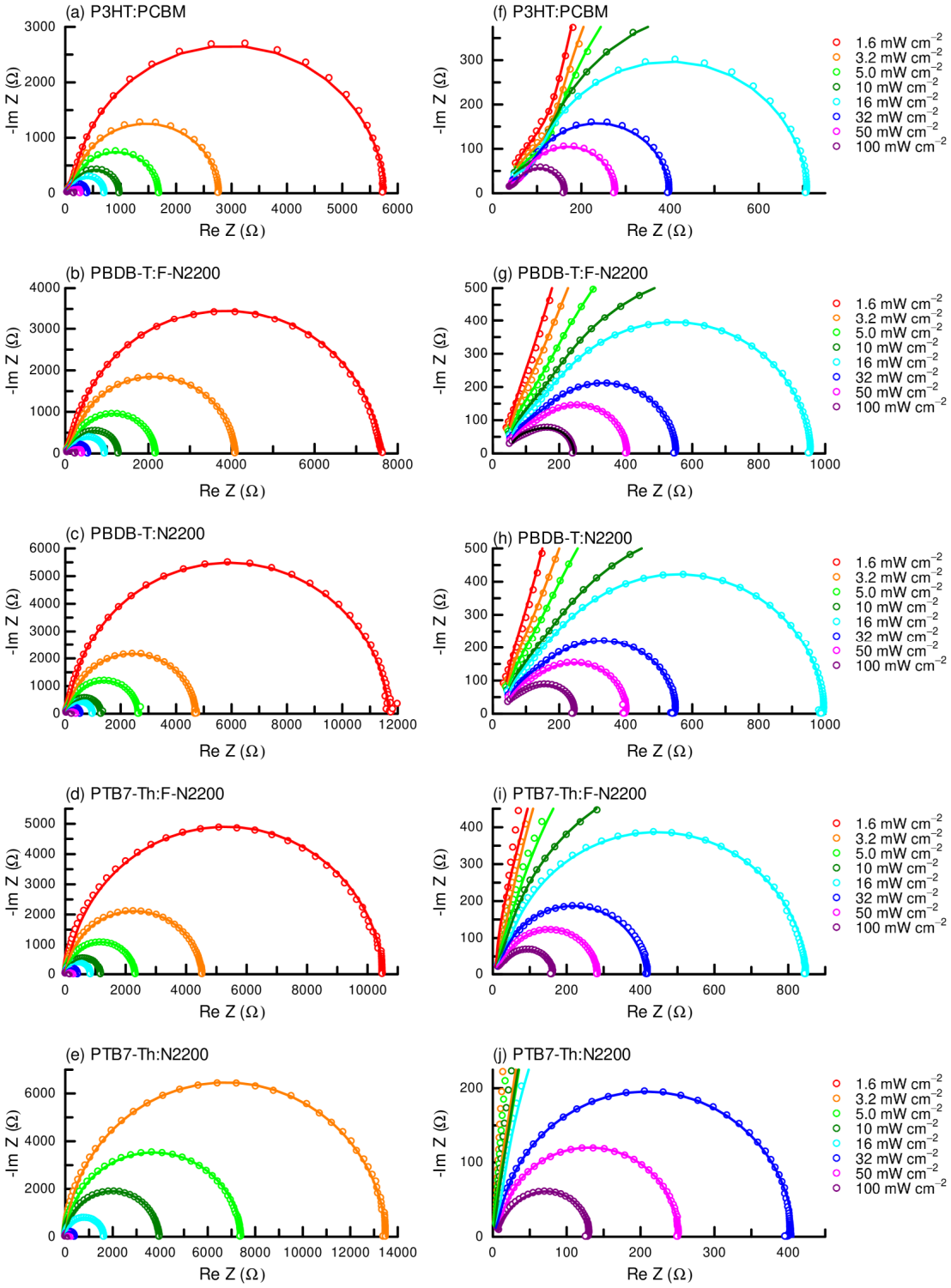

Figure S4. Impedance spectra at different illumination intensities (open-circuit conditions) for (a)(f) P3HT:PCBM, (b)(g) PBDB-T:F-N2200, (c)(h) PBDB-T:N2200, (d)(i) PTB7-Th:F-N2200, and (e)(j) PTB7-Th:N2200. (a)–(e) Complete response. (f)–(j) Detailed response under high-illumination conditions.

5. Bimolecular recombination coefficient—k_{rec}

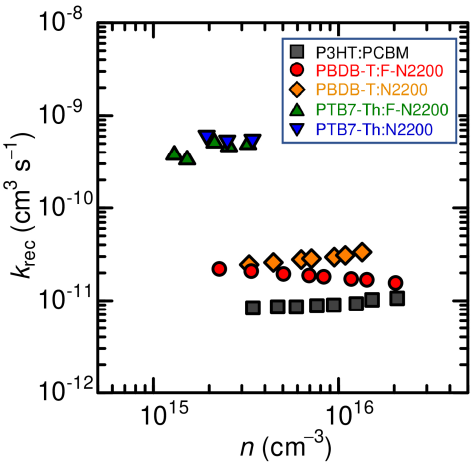

Figure S5. Bimolecular recombination coefficient (k_{rec}) as a function of the charge-carrier density (n) obtained for the devices using **Equation (10)** in the main text. Different symbols represent the results of different devices as indicated by the legends in the graph.

6. Light intensity dependence of V_{OC}

Figure S6 shows V_{OC} as a function of light intensity at 294 K for the devices. The dashed lines represent best fits to the data (symbols) for a natural logarithmic dependence of V_{OC} on light intensity with a slope of $S = nk_BT/e$, where e is the elementary charge, k_B is Boltzmann constant, T is temperature in Kelvin. The n value obtained from the slope for each device was n = 1.24 (P3HT:PCBM), 1.17 (PBDB-T:F-N2200), 1.07 (PBDB-T:N2200), 1.38 (PTB7-Th:F-N2200), and 1.18 (PTB7-Th:N2200).

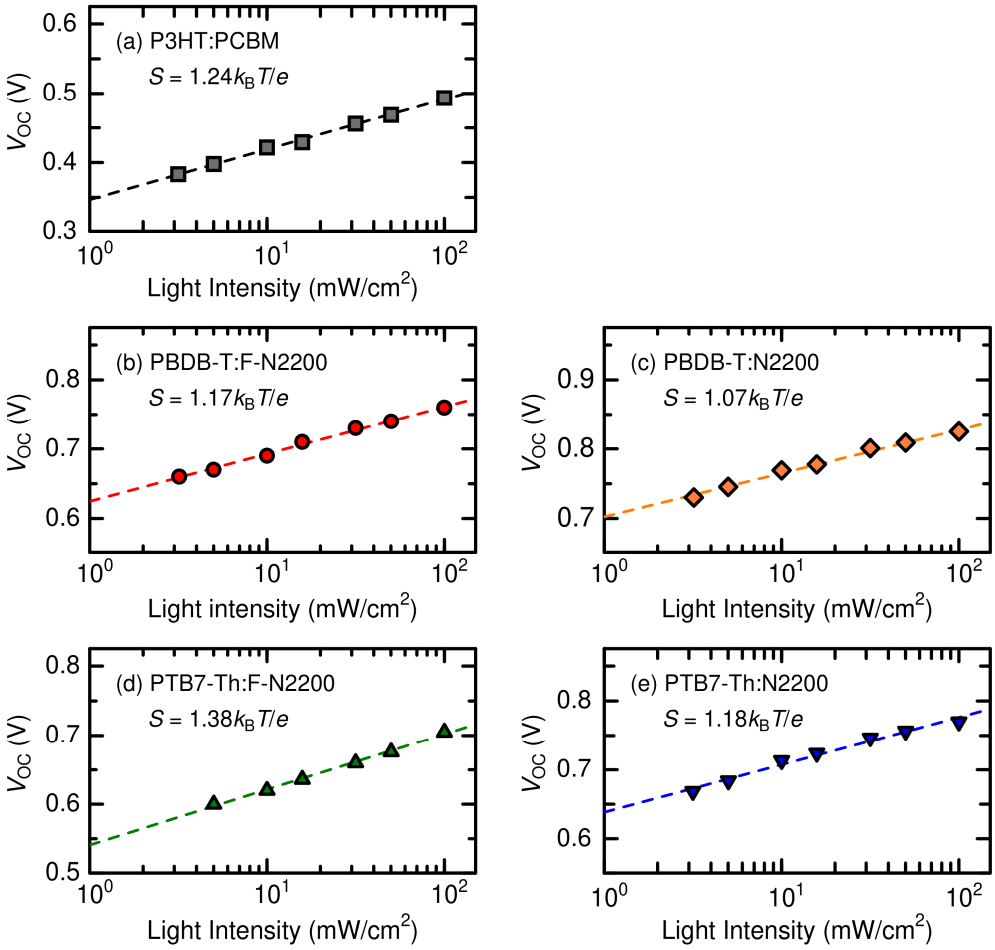

Figure S6. Open-circuit voltage (symbols) as a function of incident light intensity; (a) P3HT:PCBM, (b) PBDB-T:F-N2200, (c) PBDB-T:N2200, (d) PTB7-Th:F-N2200, and (e) PTB7-Th:N2200. The dashed lines denote linear fits to the experimental data.

7. Grazing-incidence wide-angle X-ray scattering (GWAXS) results for the P3HT neat and P3HT:PCBM blend films

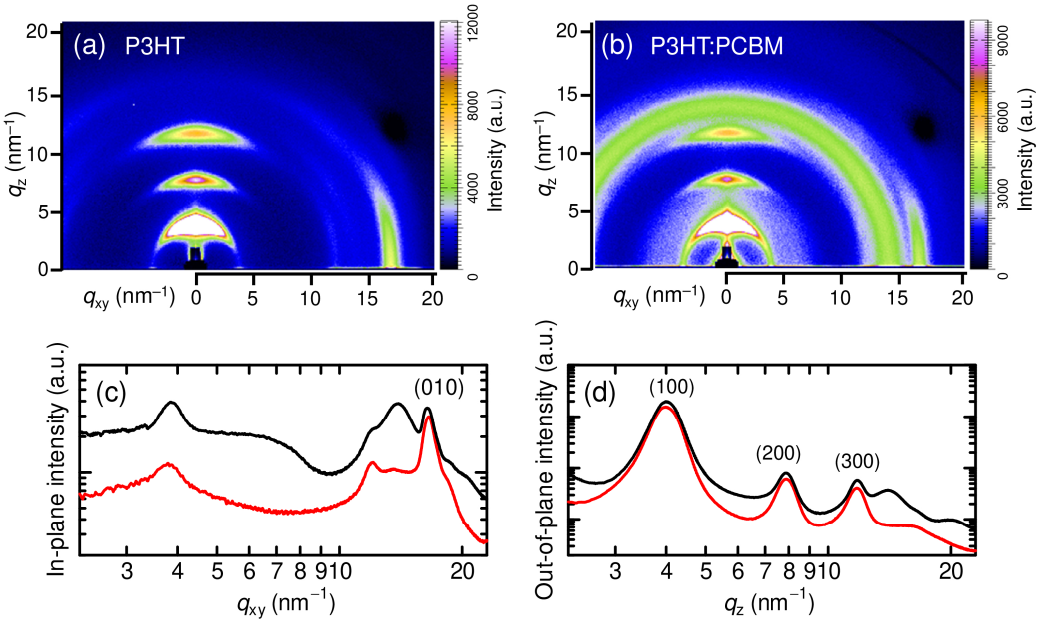

Figure S7. 2D GIWAXS patterns of the (a) P3HT neat and (b) P3HT:PCBM blend films. 1D profiles in the (c) in-plane and (d) out-of-plane directions, obtained from the 2D patterns of the P3HT neat (red lines) and P3HT:PCBM blend (black lines) films.

8. GIWAXS results for the neat films of polymer acceptors

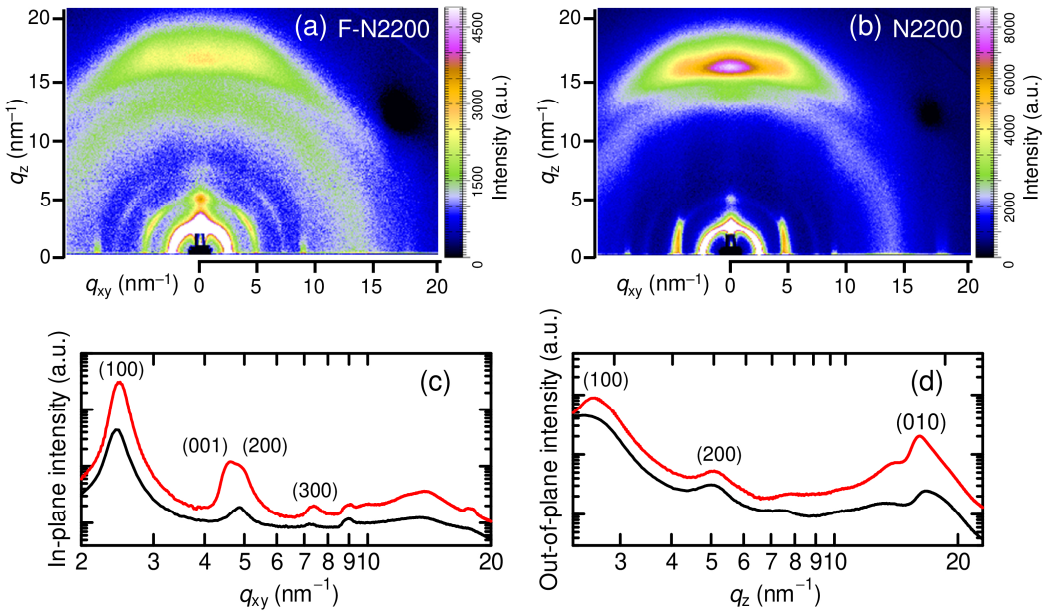

Figure S8. 2D GIWAXS patterns of the (a) F-N2200 and (b) N2200 neat films spin-coated from the chlorobenzene solution. 1D profiles in the (c) in-plane and (d) out-of-plane directions, obtained from the F-N2200 (black lines) and N2200 (red lines) 2D patterns.

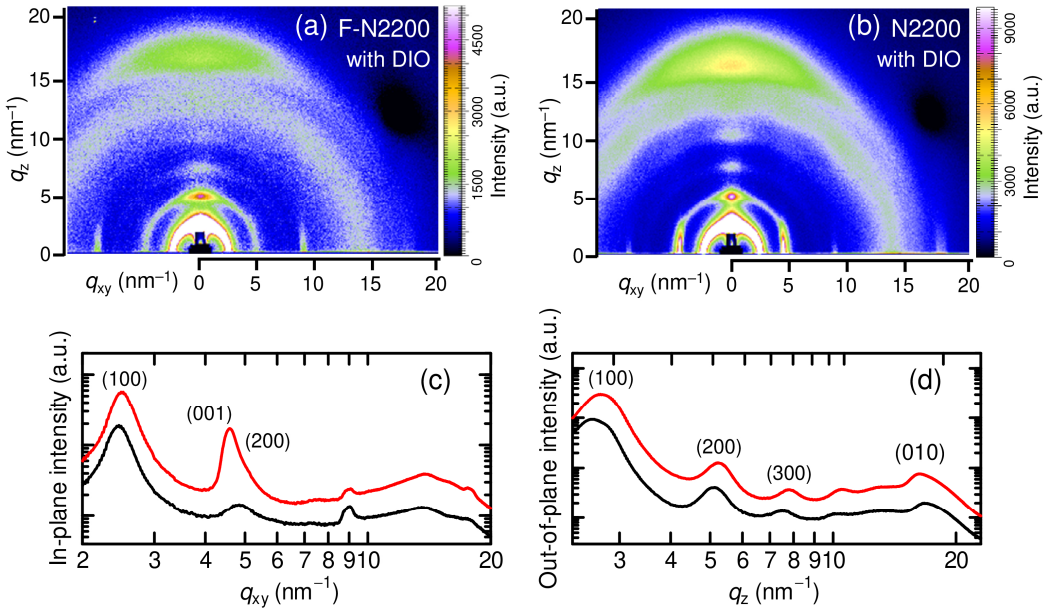

Figure S9. 2D GIWAXS patterns of the (a) F-N2200 and (b) N2200 neat films spin-coated from the chlorobenzene solution containing 0.5 wt% of DIO. 1D profiles in the (c) in-plane and (d) out-of-plane directions, obtained from the F-N2200 (black lines) and N2200 (red lines) 2D patterns.

9. Reconstruction of 1D profiles of the blend film

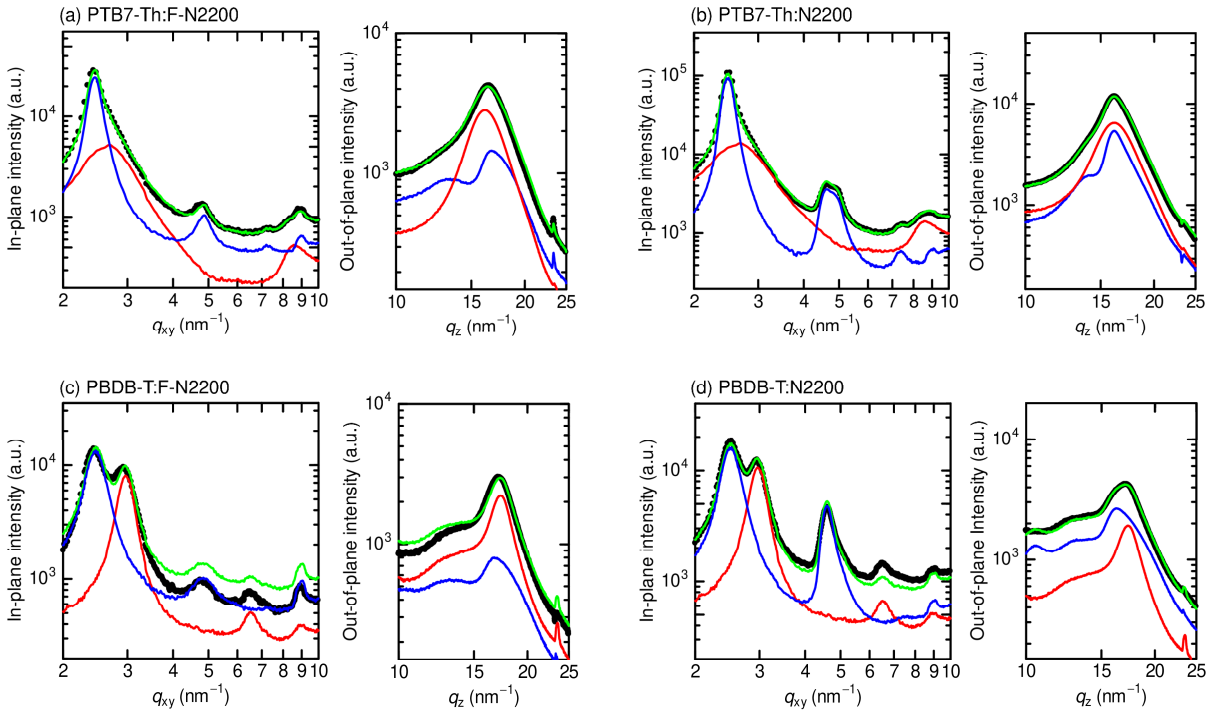

Figure S10. The black circles show the 1D profiles for the in-plane lamellar stacking and out-of-plane π–π stacking obtained from the 2D patterns of the donor:acceptor blend films: (a) PTB7-Th:F-N2200, (b) PTB7-Th:N2200, (c) PBDB-T:F-N2200, and (d) PBDB-T:N2200. The green lines represent the superposition of the profiles obtained from the individual polymer donor (red lines) and acceptor (blue lines) neat films.

Table S1. In-plane and out-of-plane GIWAXS peak parameters obtained for the P3HT neat and P3HT:PCBM blend films.

		In-plane π–π stacking				
	Index	q_{xy} (nm^{-1})	d (nm)	FWHM (nm^{-1})	L_c (nm)	N
P3HT	(010)	16.56	0.38	1.200	4.71	12.4
P3HT:PCBM	(010)	16.52	0.38	1.206	4.69	12.3

		Out-of-plane lamellar stacking				
	Index	q_z (nm^{-1})	d (nm)	FWHM (nm^{-1})	L_c (nm)	N
P3HT	(100)	4.00	1.57	0.619	9.13	5.8
	(200)	7.88	—	—	—	—
	(300)	11.76	—	—	—	—
P3HT:PCBM	(100)	4.01	1.57	0.604	9.37	6.0
	(200)	7.87	—	—	—	—
	(300)	11.76	—	—	—	—

Table S2. In-plane and out-of-plane GIWAXS peak parameters obtained for the polymer donor and acceptor neat films.

		In-plane lamellar stacking				
Polymer	Index	q_{xy} (nm^{-1})	d (nm)	FWHM (nm^{-1})	L_c (nm)	N
PBDB-T	(100)	2.97	2.12	0.352	16.07	7.6
PTB7-Th	(100)	2.68	2.35	0.947	5.97	2.5
F-N2200 w/o[a]	(100)	2.44	2.57	0.228	24.82	9.7
F-N2200 w[b]	(100)	2.46	2.56	0.348	16.26	6.4
N2200 w/o[a]	(100)	2.48	2.53	0.209	27.01	10.7
N2200 w[b]	(100)	2.51	2.51	0.333	16.99	6.8

		Out-of-plane π–π stacking				
Polymer	Index	q_z (nm^{-1})	d (nm)	FWHM (nm^{-1})	L_c (nm)	N
PBDB-T	(010)	17.32	0.36	2.439	2.32	6.4
PTB7-Th	(010)	16.19	0.39	3.782	1.50	3.9
F-N2200 w/o[a]	(010)	16.57	0.38	1.761	3.21	8.5
F-N2200 w[b]	(010)	16.62	0.38	1.934	2.92	7.7
N2200 w/o[a]	(010)	16.09	0.39	1.481	3.82	9.8
N2200 w[b]	(010)	16.14	0.39	1.917	2.95	7.6

[a] w/o: film was spin-coated from the chlorobenzene solution.
[b] w: film was spin-coated from the chlorobenzene solution containing 0.5 wt% of DIO.

Table S3. In-plane GIWAXS peak parameters calculated for the blend films and the constituent donor and acceptor neat films. The values for the neat films are shown in square brackets.

Blend	Index	q_{xy} (nm^{-1})	d (nm)	L_c (nm)	N
PTB7-Th : F-N2200	Donor (100)	2.71 [2.68]	2.32 [2.35]	8.57 [5.97]	3.7 [2.5]
	Acceptor (100)	2.43 [2.44]	2.59 [2.57]	23.7 [24.8]	9.2 [9.7]
PTB7-Th : N2200	Donor (100)	2.83 [2.68]	2.22 [2.35]	8.23 [5.97]	3.7 [2.5]
	Acceptor (100)	2.49 [2.48]	2.52 [2.53]	29.4 [27.0]	11.7 [10.7]
	Acceptor (001)	4.62 [4.58]	1.36 [1.37]	15.2 [15.9]	11.1 [11.6]
PBDB-T : F-N2200	Donor (100)	2.94 [2.97]	2.14 [2.12]	11.4 [16.1]	5.3 [7.6]
	Donor (001)	6.56 [6.54]	0.96 [0.96]	8.29 [8.75]	8.7 [9.1]
	Acceptor (100)	2.44 [2.46]	2.58 [2.56]	17.8 [16.3]	6.9 [6.4]
PBDB-T : N2200	Donor (100)	2.96 [2.97]	2.12 [2.12]	14.6 [16.1]	6.9 [7.6]
	Donor (001)	6.55 [6.54]	0.96 [0.96]	7.94 [8.75]	8.3 [9.1]
	Acceptor (100)	2.50 [2.51]	2.51 [2.51]	18.1 [17.0]	7.2 [6.8]
	Acceptor (001)	4.60 [4.59]	1.37 [1.37]	14.6 [18.8]	10.7 [13.7]